ACS APPLIED MATERIALS & INTERFACES

www.acsami.org Research Article

Natural Small Biological Molecule Based Supramolecular Bioadhesives with Innate Photothermal Antibacterial Capability for Nonpressing Hemostasis and Effective Wound Healing

Xiang Ke, Shuxian Tang, Hao Wang, Yusong Cai, Zhiyun Dong, Mingjing Li, Jiaojiao Yang, Xinyuan Xu, Jun Luo,* and Jianshu Li*

Cite This: https://doi.org/10.1021/acsami.2c17415 Read Online

ACCESS | Metrics & More | Article Recommendations | Supporting Information

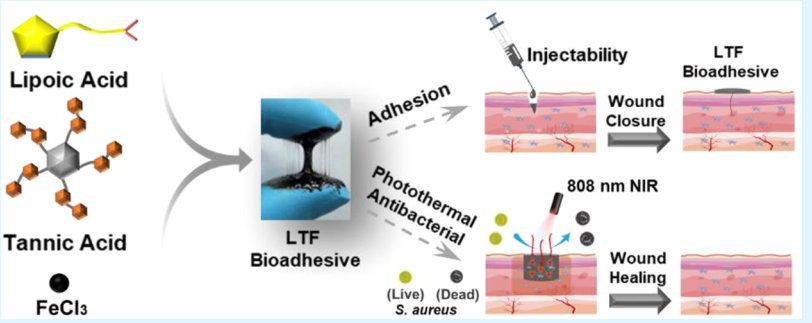

ABSTRACT: Bioadhesives with immediate wound closure, efficient hemostasis, and antibacterial properties that can well integrate with tissue are urgently needed in wound management. Natural small biological molecule based bioadhesives hold great promise for manipulating wound healing by taking advantage of integrated functionalities, synthetic simplification, and accuracy, cost efficiency and biosafety. Herein, a natural small biological molecule based bioadhesive, composed of natural small biological molecules (α-lipoic acid and tannic acid) and a small amount of ferric chloride, was prepared via an extremely simple and green route for wound management. In this system, covalent and noncovalent interactions between each component resulted in the self-healing supramolecular bioadhesive. It possessed appropriate wet-tissue adhesion, efficient nonpressing hemostasis and free radical scavenging abilities. More importantly, the interaction between tannic acid and Fe^{3+} endowed the bioadhesive with innate and steady photothermal activity, which showed excellent photothermal bactericidal activity to both *E. coli* and *S. aureus*. The bioadhesive promoted wound healing for linear and circular wounds *in vivo*, especially for infectious wounds under near-infrared (NIR) irradiation. This bioadhesive will have promising value as a safe and effective antimicrobial adhesive for infectious wound management.

KEYWORDS: *natural small molecule, supramolecular bioadhesives, photothermal antibacterial, hemostasis, wound healing*

1. INTRODUCTION

Wound management is a fundamental healthcare concern because of numerous traumatic injuries and chronic wounds, especially acute hemorrhage and pathogen infection cases.[1−3] Conventional wound closure strategies, including sutures and staples, have been extensively used to manipulate the wound repair process in clinical care, while these strategies are often associated with secondary trauma, fluid leakage and poor antibacterial activity.[4,5]

Bioadhesives have been developed as alternatives for promoting the wound healing process, such as fibrin glue and cyanoacrylate.[6] They can adhere to tissue surfaces and integrate with tissue by forming chemical cross-links and mechanical interlocks for wound closure with less pain and scar than sutures and staples,[7,8] while some disadvantages of current bioadhesives, such as toxic monomers/initiators, complicated preparation process, and poor adhesion strength, affect their clinical outcomes.[9] In addition, acute hemorrhage and infectious contaminations after trauma are of concern. Once bacterial infection occurs, severe wound inflammation, prolonged wound healing, and even fatal consequences may happen.[10,11] Thus, developing bioadhesives with immediate wound closure, efficient hemostasis, and antibacterial properties that can well integrate with tissue are urgently needed in wound management, especially for trauma emergencies.

Received: September 26, 2022
Accepted: November 3, 2022

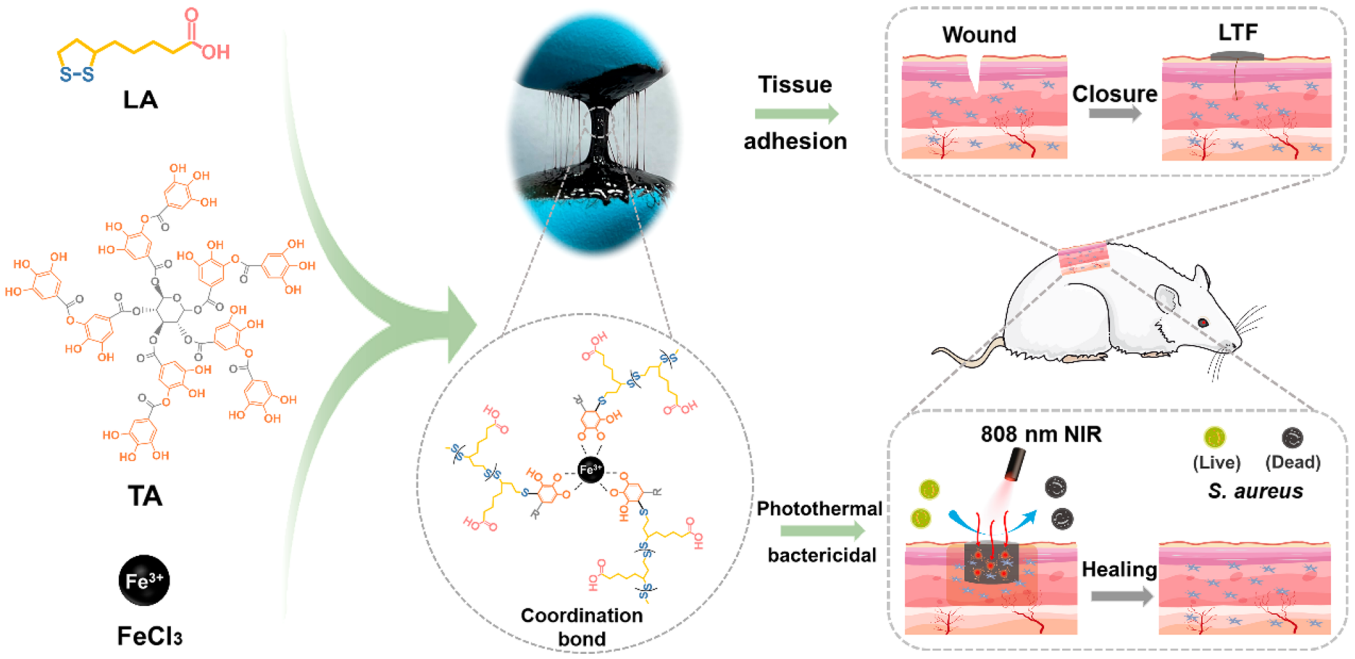

Figure 1. Schematic illustration of the preparation process of the LTF supramolecular bioadhesive and its application in wound management. The LTF supramolecular bioadhesive has good photothermal performance due to the catechol−metal coordination bonds, which endow it with excellent photothermal antibacterial properties and are beneficial to wound healing.

Tannic acid, a commonly used plant polyphenol with rich catechol and pyrogallol groups, has good biocompatibility, strong tissue adhesiveness, inherent hemostatic, antioxidant and mild antibacterial potentials, as well as particular photothermal activity when combined with Fe^{3+} to kill bacteria.[12,13] Therefore, it has been widely used as an effective adhesive moiety to prepare mussel-inspired bioadhesives by combing with macromolecules or modifying macromolecules.[14,15] However, toxic substances, complex modification/synthesis, or the uncontrolled molecular structure of polymeric feedstocks may affect the biocompatibility, composition accuracy, and stability of these bioadhesives and therefore hinders them from further clinical application.[16] In addition, due to the mild antibacterial capacity, these mussel-inspired adhesives commonly required additional antibacterial agents (e.g., antibiotic and metal nanoparticles) for efficient bacteria inactivation in bacterial-infectious cases, while the risk of uncontrolled drug release, potential drug resistance, and side effect remains a notable problem.[17,18] Moreover, the addition of antibacterial agents is usually harmful to the intrinsic properties (e.g., adhesiveness) of the bioadhesives.[19]

To overcome these problems, natural small biological molecule based bioadhesives would be a promising solution by taking advantage of integrated functionalities, synthetic simplification, structure accuracy, cost efficiency and biosafety.[20] Specifically, the development of supramolecular bioadhesives by self-assembly of natural small biological molecules with innate nonpharmacological physical antibacterial potential can combine biosafety and highly efficient bacteria inactivation for infectious wound repair and tissue regeneration.[21,22]

α-Lipoic acid, a biocompatible natural small molecule and an essential coenzyme occurring in aerobic metabolism *in vivo*, contains a five-membered ring-containing disulfide bond and a carboxyl group in its molecular structure.[23,24] Our previous study revealed that α-lipoic acid can incorporate tannic acid and ferric chloride to fabricate a high-performance universal underwater adhesive.[25] More importantly, the interaction between tannic acid and Fe^{3+} within the adhesive is supposed to endow the bioadhesive with potential photothermal antibacterial activity, which might be an efficient and cost-effective nonpharmacological physical therapy strategy for antibacterial wound management.[26,27] However, there was very little in-depth research to investigate the potential of this natural small biological molecule based bioadhesive in promoting wound healing.

Therefore, in this work, we constructed the bioadhesive (referred to as LTF) based on α-lipoic acid, tannic acid, and ferric chloride via a facile and green route and applied it to promote wound closure, especially in bacterial-infectious wound models (Figure 1). The bioadhesive showed not only instant and reliable adhesion to various wet tissues but also efficient hemostasis and free radical scavenging abilities. More importantly, the bioadhesive possessed innate and steady photothermal activity. Antibacterial tests *in vitro* demonstrated that the bioadhesive could highly efficiently inactivate bacteria (>99% for both *Escherichia coli* and *Staphylococcus aureus*) under 808 nm NIR irradiation. For differently shaped wounds (i.e., linear and circular wounds) *in vivo*, the bioadhesive can be manipulated to render appropriate adhesion to skin tissue and promote the wound healing process, especially for infectious wounds under NIR irradiation. The promoted wound closure effect of the bioadhesive can be mainly attributed to its appropriate adhesion strength, efficient hemostasis and free radical scavenging abilities, as well as synergistic photothermal and polyphenol antibacterial effects. This work provided a natural small molecule based bioadhesive with innate photothermal activity for effective wound treatment.

2. EXPERIMENTAL SECTION

2.1. Materials. Lipoic acid (LA) was obtained from Macklin Biochemical Co., Ltd. (Shanghai, China); tannic acid (TA) and 1,1-

https://doi.org/10.1021/acsami.2c17415
ACS Appl. Mater. Interfaces XXXX, XXX, XXX−XXX

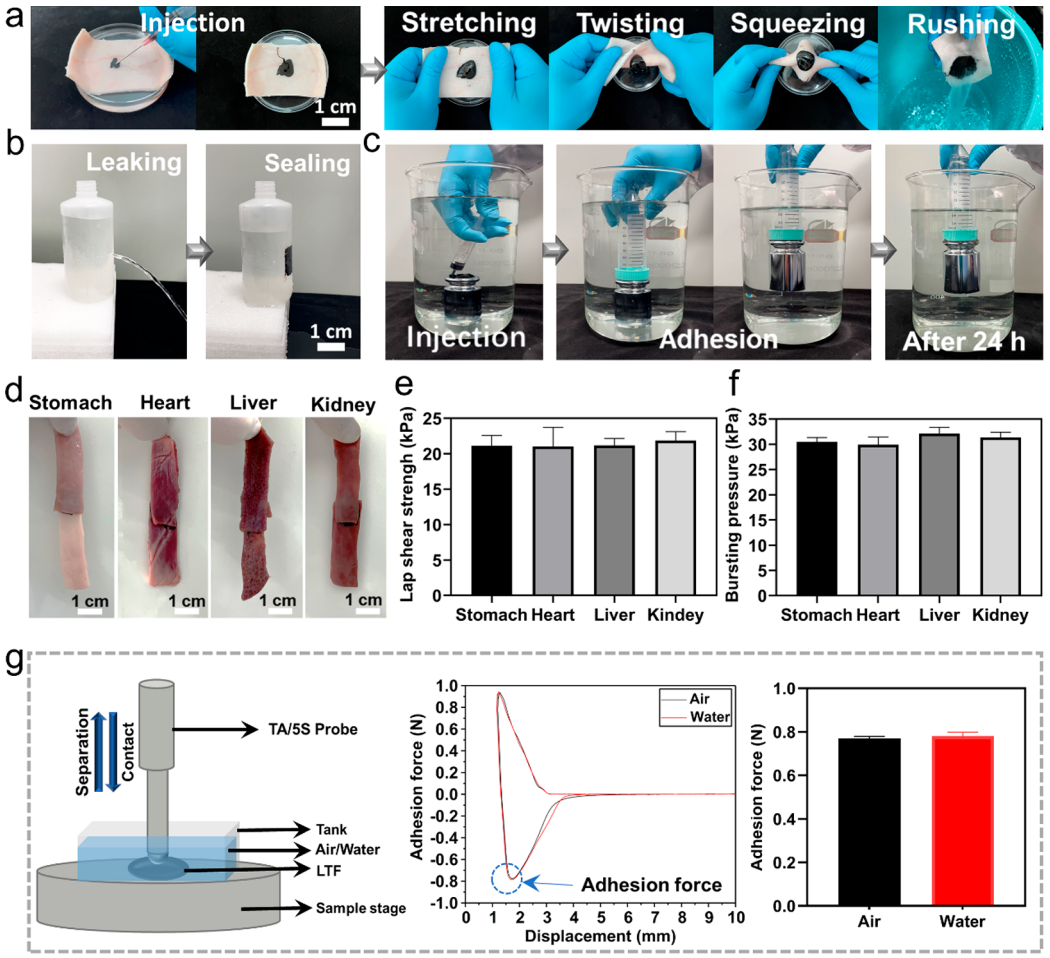

Figure 2. Adhesion performance. (a) LTF supramolecular bioadhesive can be injected from an 18G needle and can withstand stretching, twisting, squeezing, and water flushing. (b) Thin PET film with the LTF bioadhesive on its surface can seal the hole in the plastic bottle and completely prevent water leakage. (c) LTF supramolecular bioadhesive could be injected underwater and bear a weight weighing 500 g (adhesion area: 3 cm in diameter). (d) LTF supramolecular bioadhesives can join different wet tissue samples. (e) Lap shear strength and (f) bursting pressure of the LTF supramolecular bioadhesive for wet tissue samples. (g) Scheme of the adhesion force test and the adhesion force of the LTF supramolecular bioadhesive in different conditions. The values were presented as the mean ± SD.

diphenyl-2-picrylhydrazyl (DPPH) were purchased from Aladdin Biochemical Technology Co., Ltd. (Shanghai, China). Ferric chloride ($FeCl_3$) was purchased from Adamas-beta Reagent Co., Ltd. (Shanghai, China).

2.2. Synthesis of the LTF Supramolecular Bioadhesive. As shown in Figure 1, LA (1.25 g) was heated at 150 °C for 5 min, and then TA (0.05 g) and $FeCl_3$ (0.02 g) were sequentially added under the same heating and stirring condition for 15 min. The resulting viscous mixture was cooled down at room temperature (25 ± 1 °C) to obtain the LTF supramolecular bioadhesive.

2.3. Characterization of the LTF Supramolecular Bioadhesive. ^{1}H nuclear magnetic resonance (^{1}H NMR) spectra and ^{13}C nuclear magnetic resonance (^{13}C NMR) spectra were obtained using DMSO-d6 as the solvent at room temperature (Bruker Ascend 400 MHz NMR instrument, Germany). X-ray diffraction (XRD, Ultima IV, Rigaku, Japan) analysis was performed at room temperature with 2θ range of 5−80° in steps of 0.02°. Fourier transform infrared (FT-IR) spectra (Nicolet 6700, Thermo Scientific, USA) were analyzed with the wavenumber ranging from 500 to 4000 cm^{-1} at a resolution of 4 cm^{-1}. The thermal behaviors of LA, TA, and LTF were investigated using differential scanning calorimetry (DSC) (SDT-Q600, TA Instruments, USA) at a heating temperature ranging from 35 to 900 °C and a heating rate of 10 °C min^{-1} under nitrogen atmosphere. The surface micromorphology of the LTF sample was observed using scanning electron microscope (SEM, Apreo S HiVoc, USA) at an acceleration voltage of 10 kV.

2.4. Adhesion Force Test. The adhesion force in diverse conditions was measured using a texture analyzer (TA. Xtc-20; Bosin Tech, Shanghai) at 37 °C (Figure 2g). Specifically, LTF was poured into a PTFE mold (2.0 mm in thickness and 10 mm in diameter). Then, the PTFE mold was placed in a tank to provide diverse test conditions (dry and underwater). In the constant compression mode, a TA/5S probe with a speed of 1 mm s^{-1} was brought into contact with the LTF sample from a fixed force (1 N) and then retracted when the displacement of the plate reached a fixed value (10 mm away from the sample stage surface). The maximum force applied to separate the plate from the LTF sample was set as the adhesion force. Three samples were tested for each condition.

2.5. Rheological Behaviors. The rheological behaviors of LTF were measured using the rheometer (MCR302, Anton Paar, Austria) with an 8 mm plate at 37 °C. The time sweep test was conducted from 0 to 5 min at a fixed strain of 1% and frequency of 1 Hz. The strain sweep test was performed from 0.1 to 1000% strain at a fixed frequency of 1 Hz. The temperature sweep test was performed from 0 to 45 °C at a fixed frequency of 1 Hz and strain of 1%. The viscosity test was conducted by increasing the shear rate from 1 to 1000 s^{-1} at a temperature of 37 °C. The alternate step strain sweep test was performed by applying a 1% strain and 400% strain at a fixed frequency of 1 Hz and a temperature of 37 °C.

2.6. Lap Shear Test. According to the modified method ASTM F2255−05, fresh tissues including the stomach, heart, liver, and kidney of pigs were selected as the substrates to evaluate the tissue

https://doi.org/10.1021/acsami.2c17415
ACS Appl. Mater. Interfaces XXXX, XXX, XXX−XXX

adhesion properties of the LTF supramolecular bioadhesive.[28,29] Different tissues were cut with dimensions of 3 cm × 1 cm × 2 mm. The LTF supramolecular bioadhesive was evenly spread between two pieces of the same substrate, with an overlap area of 1 cm × 1 cm. Then, finger pressure was applied for approximately 15 s. Subsequently, the shear strength required to detach the two substrates was recorded using a universal mechanical testing instrument (HZ-1004B, China) with a load cell of 200 N and a fixed extension speed of 100 mm min^{-1}. At least three samples were tested for each substrate.

2.7. Burst Pressure Test. The fresh tissues including the stomach, heart, liver, and kidney of pigs were selected as the substrates to evaluate the water-proof capacities of the LTF supramolecular bioadhesive.[30,31] Different tissues (Φ = 26 mm, H = 2 mm) were fixed on a measurement device with water. Then a circular incision with a diameter of 2 mm was made by a scalpel at the tissue center. Subsequently, the LTF supramolecular bioadhesive was directly attached to the incision site. The value of the bursting pressure was recorded by a digital meter until the pressure began to decrease. Three samples were tested for each tissue.

2.8. Cytocompatibility and Proliferation *In Vitro*. L929 cells were chosen to estimate the cytocompatibility of the LTF supramolecular bioadhesive. First, the L929 cells were cultured in a complete alpha modified Eagle's medium (α-MEM) medium (10% fetal bovine serum and 1% penicillin−streptomycin) for 24 h at 37 °C with 5% CO_2. Different amounts of the LTF supramolecular bioadhesive were coated on the surface of Ti plates and put into a 24-well plate. Then the L929 cells were seeded with a density of 5 × 10^4 cells per well and incubated at 37 °C with 5% CO_2 for 24 h. Subsequently, the cell counting kit-8 (CCK-8) assay kit (Med Chem Express, USA) was employed to measure cell viability and cell proliferation after 1, 3, 5, and 7 days, respectively. Briefly, 500 μL of CCK-8 solution was added to each well and cocultured with L929 cells at 37 °C for 3 h. Then, the optical density (OD) was measured by a microplate reader (Spectra Max ABS, USA) at 450 nm. Cell viability (CV) was calculated according to the following eq 1:

$$CV(\%) = (OD_{ex} - OD_b)/(OD_c - OD_n) \times 100\% \quad (1)$$

where OD_{ex} is the OD value of experimental groups, OD_b is the OD value of background groups (pure LTF bioadhesive with α-MEM complete medium), OD_c is the OD value of the control group (cells in α-MEM complete medium without LTF bioadhesive), and OD_n is the OD value of blank group (only α-MEM complete medium).

2.9. Cell Staining *In Vitro*. Live and dead L929 cells cocultured with the LTF supramolecular bioadhesive on first day and seventh day were stained by the fluorescein diacetate (FDA) and propidium iodide (PI) to further evaluate the cytocompatibility of the LTF bioadhesive *in vitro*.[32] Briefly, L929 cells cultured with the LTF supramolecular bioadhesive after different time points were stained by FDA (10 μg mL^{-1}) and PI (16 μg mL^{-1}) for 30 min. Then the cells were washed with phosphate buffer saline (PBS) and the live/dead cells were observed by a fluorescence microscope (IX-71, Olympus, Japan). The nuclei and actin cytoskeletons of the L929 cells cocultured with the LTF supramolecular bioadhesive after 24 h were stained by 4,6-diamidino-2-phenylindole (DAPI) and rhodamine-labeled phalloidin to investigate the morphology of the L929 cells. Briefly, the L929 cells were immobilized by 4% paraformaldehyde for 20 min and then permeabilized by 0.1% Triton X-100 for 5 min. Subsequently, the cells were stained with rhodamine-labeled phalloidin (1 μg mL^{-1}) for 30 min and DAPI (5 μg mL^{-1}) for 10 min. Then the cells were washed with PBS and the morphology of the L929 cells was observed by a fluorescence microscope (IX71, OLYMPUS, Japan).

2.10. Photothermal Performance. The photothermal performance of the LTF supramolecular bioadhesive was tested by continuously irradiating the adhesive samples using an 808 nm NIR laser (BWT, DS3−51412−0110, Beijing) with different power densities for 5 min. The changes in temperature and thermal images were recorded by a thermal imaging camera (Testo, 885, Germany).

2.11. Photothermal Antibacterial Test *In Vitro*. The photothermal antibacterial property of the LTF supramolecular bioadhesive was evaluated by using *S. aureus* (CMCC 26003) and *E. coli* (ATCC 25922) *in vitro*.[27] Briefly, 5 mg of the LTF bioadhesive was coated on each Ti plate and put into a 24-well plate, and 100 μL of bacterial suspension (10^7 CFU mL^{-1}) of either *S. aureus* or *E. coli* was added to each sample. Then, the 808 nm NIR laser was used to irradiate the LTF bioadhesive with 1.5 W cm^{-2} power density for 10 min, and 900 μL of nutrient broth (NB) medium was introduced into each well. The samples were incubated at 37 °C for 24 h. Subsequently, the bacterial suspension in the 24-well plate was transferred into a 96-well plate (100 μL per well) to record the optical density (OD) at 600 nm by means of a microplate reader (Spectra Max ABS, USA). Three samples were tested for each experimental group. The bactericidal ratio (BR) was calculated according to the following eq 2:

$$BR(\%) = 100\%\text{-}(OD_{ex} - OD_b)/(OD_c - OD_n) \times 100\% \quad (2)$$

where OD_{ex} is the OD value of the experimental groups, OD_b is the OD value of the background group (NB medium with LTF bioadhesive sample), and OD_c and OD_n are the OD values of the control group (only bacterial suspension) and the blank group (only NB medium), respectively.

After that, 100 μL of bacterial suspensions cocultured with the LTF supramolecular bioadhesive for 24 h were evenly spread on agar plates and continued to incubate at 37 °C for 24 h. Finally, colonies of either *S. aureus* or *E. coli* on the agar plates were observed and recorded by a digital camera.

2.12. Free Radical Scavenging Ability. The DPPH radical scavenging ability of the LTF supramolecular bioadhesive was evaluated according to the previously established method.[33] Briefly, 2 mL of 0.2 mM DPPH/ethanolic solution was incubated with 800 μL of the ethanolic solution with different concentrations of the LTF supramolecular bioadhesive. Then, the volume of the mixture solution was fixed at 4 mL and incubated in dark at 37 °C for 30 min. Subsequently, the absorbance of the mixture solution was tested at 517 nm against a blank solution using vis−UV (TU-1901, China). Three samples were tested for each experimental group. The DPPH radical scavenging ratio (%) was calculated using the following eq 3:

$$\text{DPPH radical scavenging ratio}(\%) = (1 - A_{ex517}/A_{c517}) \times 100\% \quad (3)$$

where A_{ex517} is the absorbance of the mixture solution with different concentrations of LTF and A_{c517} is the absorbance of 0.2 mM DPPH/ethanolic solution.

2.13. *In Vitro* Hemostatic Ability Tests. All studies in rats were approved by the Animal Ethics Committee of Chengdu Dossy Experimental Animals Co., Ltd., China. Sprague−Dawley (SD) rat hemorrhaging models of tail, heart, and liver were carried out to evaluate the hemostatic capacity of the LTF supramolecular bioadhesive.[34] For the hemorrhaging tail model, female SD rats weighing 200−250 g were randomly divided into 3 groups (each group contained 3 mice) and were anesthetized with 3% pentobarbital sodium. Then after sterilization with 75% ethanol, the tail was cut off with a length of 2 cm (recorded as the start time). Immediately, the bleeding ends of the tail were treated with the LTF supramolecular bioadhesive and gauze, respectively. The weight of the materials in each group was weighed in advance. The time when the wound stopped bleeding was recorded as the hemostasis time. The material in each group was weighed again to calculate the mass of the blood.[15] No treatment was performed in the blank group. Images of the bleeding site were recorded by a digital camera. For the liver bleeding model,[34] female SD rats weighing 200−250 g were anesthetized with 3% pentobarbital sodium. After that, the abdominal surgery was performed to expose the heart and the heart was punched with an 18G needle to initiate bleeding. Immediately, the LTF supramolecular bioadhesive was coated evenly on the bleeding site. Images of the bleeding site were recorded by a digital camera. For the liver bleeding model,[35] female SD rats weighing 200−250 g were anesthetized as described above. After that, the abdominal surgery was performed to

https://doi.org/10.1021/acsami.2c17415
ACS Appl. Mater. Interfaces XXXX, XXX, XXX−XXX

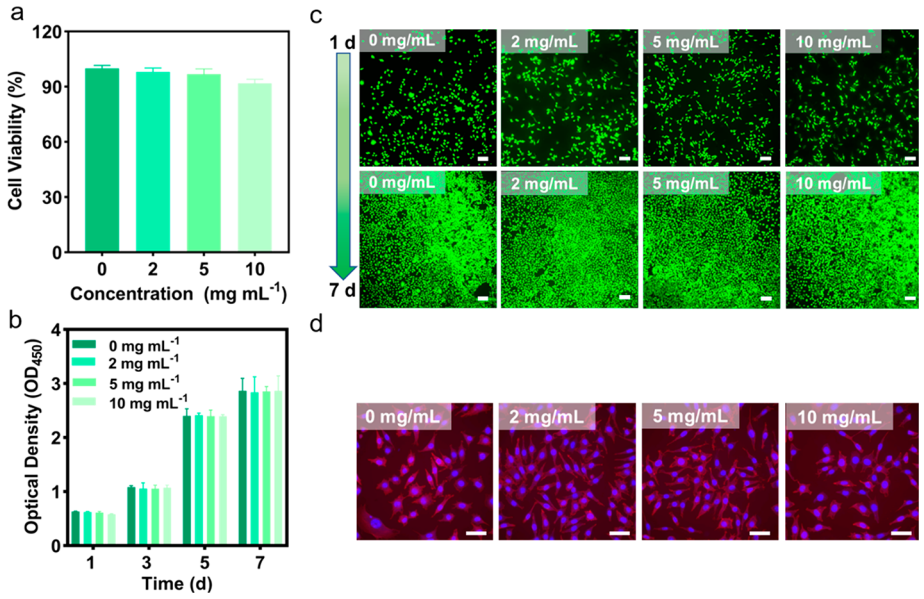

Figure 3. Cytocompatibility. (a) Cytotoxicity and (b) proliferation of the LTF supramolecular bioadhesive for L929 cells. The values are presented as the mean ± SD (c) Representative live/dead images of L929 cells incubated with the LTF supramolecular bioadhesive for 1 and 7 days, respectively. Scale bar = 100 μm. (d) Representative morphology images of L929 cells incubated with the LTF supramolecular bioadhesive for 1 day. Scale bar = 50 μm.

expose the liver, and the liver was also punched with an 18G needle to initiate bleeding. Immediately, the LTF supramolecular bioadhesive was coated evenly on the bleeding site. Images of the bleeding site were recorded by a digital camera. For the intestine leakage model,[36] female SD rats weighing 200−250 g were anesthetized as described above. After that, the abdominal surgery was performed to expose the intestine. The intestine was taken out, and a surgical incision was created with an 18G needle. Brilliant Blue FCF-stained normal saline was injected into the exposed intestine to obtain an obvious fluid leakage from the surgical incision. Then the LTF supramolecular bioadhesive was applied on the incision site. Images of the leakage site were recorded by a digital camera.

2.14. Wound Closure Study *In Vivo*. Female SD rats weighing 200−250 g were randomly divided into 3 groups (each group contained 9 mice for three time points) including the blank group, suture group, and LTF group.[37] 3% pentobarbital sodium was intraperitoneally injected for anesthesia. Then the skin wound model with a length of 20 mm was established on the back of each rat. The LTF supramolecular bioadhesive was employed to directly close the wound. The nonresorbable suture was used to close the wound in the suture group and no treatment was performed in the blank group. On the fifth, 10th, and 15th day, wound images were recorded by a digital camera, and the wound closure area was calculated to evaluate the wound healing process. In addition, the wound tissues on days 5, 10, and 15 were collected and fixed with 4% paraformaldehyde for H&E staining.

2.15. Wound Healing Study *In Vivo*. Female SD rats weighing 200−250 g were randomly divided into 3 groups (each group contained 9 mice for three time points) including the control group, the LTF-treated group without NIR, and the LTF-treated group with NIR.[26] 3% pentobarbital sodium was intraperitoneally injected for anesthesia. Then the full-thickness skin wound model with a diameter of 20 mm was established on the back of each rat and treated with 100 μL of *S. aureus* suspension (10^6 CFU mL^{-1}). Then the LTF supramolecular bioadhesive was coated on the wound. In the LTF-treated group with NIR, the 808 nm laser (1.5 W/cm^{-2}) was used to irradiate the adhesive in situ for 10 min. No treatment was performed in the blank group. On days 5, 10, and 15, wound images were recorded by a digital camera, and the wound closure area was calculated to evaluate the wound healing process. In addition, the wound tissues on days 5, 10, and 15 were collected and fixed with 4% paraformaldehyde, and then were used for H&E staining and Masson's staining.

3. RESULTS AND DISCUSSION

3.1. Preparation and Characterization of the LTF Supramolecular Bioadhesive. According to our previous research, the LTF supramolecular bioadhesive was prepared by coheating LA, TA, and ferric chloride ($FeCl_3$). The weight ratio of LA to TA was 25:1, and the molar ratio of LA to $FeCl_3$ was 50:1 as this formulation showed excellent comprehensive performance, such as good ductility, self-healing property, and instant and strong adhesion strength, which were desired in wound healing.[25] Details were available in the Experimental Section. Relevant physicochemical characterizations were conducted with NMR, FT-IR, XRD, and DSC to obtain information on the bioadhesive. These results (Figures S1−S5) demonstrated that LA was mediated by TA and Fe^{3+} to realize the thermally induced ring-opening polymerization.[37−40] In this system, LA underwent the thermal-initiated ring-opening polymerization and the TA was utilized as a radical scavenger to suppress the ring-closing reaction of LA initiated by live terminal diradicals. Meanwhile, Fe^{3+} facilitated the dynamic property by coordinating with phenolic hydroxyl in TA and carboxyl in LA.[25,37,38] In addition, as shown in the SEM image (Figure S6), the bioadhesive exhibited a fine texture.

According to the results of the rheological behavior test, the LTF supramolecular bioadhesive displayed the shear-thinning, temperature-sensitive, and self-healing properties (Figures S7 and S8), which was due to the existence of hydrogen bonds, dynamic covalent disulfide bonds, and coordination bonds in the three-dimensional supramolecular networks of the LTF bioadhesive.[38,41−43] Compared with preformed bioadhesives,[44,45] the shear-thinning property endowed the LTF supramolecular adhesive with good injectability for convenient usage in clinical application, especially for minimally invasive surgeries.[46,47] The self-healing property of the bioadhesive would facilitate repeated wound closure as the closed wound

https://doi.org/10.1021/acsami.2c17415
ACS Appl. Mater. Interfaces XXXX, XXX, XXX−XXX

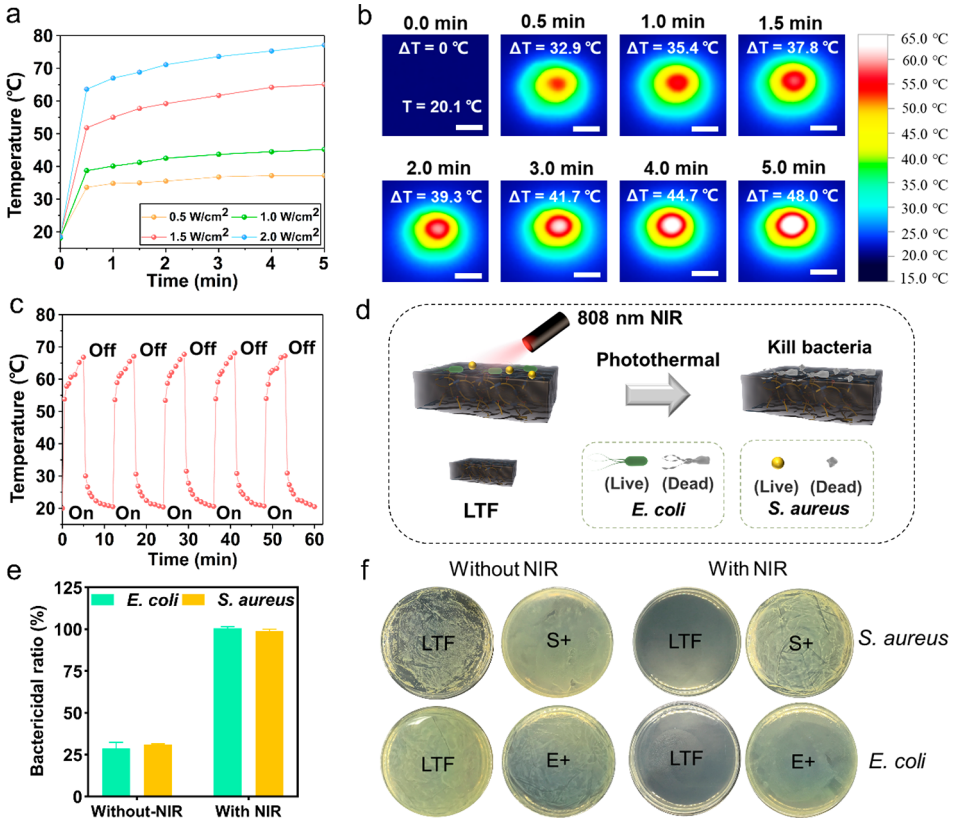

Figure 4. Photothermal antibacterial performance. (a) Changes in temperature of the LTF supramolecular bioadhesive under different power densities of 808 nm NIR irradiation. (b) Thermal images of the LTF supramolecular bioadhesive under 808 nm NIR irradiation (1.5 W cm^{-2}). Scale bar = 2 mm. (c) On/off cycle test of the LTF supramolecular bioadhesive under 808 nm NIR irradiation (1.5 W cm^{-2}). (d) Schematic diagram of the photothermal antibacterial performance of the LTF supramolecular bioadhesive. (e) Bactericidal ratios against *E. coli* and *S. aureus* of the LTF supramolecular bioadhesive with and without 808 nm NIR irradiation. The values are presented as the mean ± SD. (f) Photographs of agar plates cocultured with *S. aureus* and *E. coli* suspensions with and without 808 nm NIR irradiation for 24 h.

may be reopened due to frequent movement during wound healing.[48,49]

As shown in Figure 2a and Video S1, the LTF supramolecular bioadhesive could be easily injected underwater and adhere to fresh porcine skin tissue instantly. The porcine skin with the LTF bioadhesive could also withstand the stretching, twisting, squeezing, and even flushing by water flow, due to the covalent bond, hydrogen bond, and $\pi-\pi$ interaction generated between the LTF bioadhesive and the surface of porcine skin that achieved the superior adhesion.[8,50,51] In addition, as shown in Figure 2b and Video S2, due to the universal adhesion property of polyphenol, the LTF bioadhesive could coat on a thin PET film to seal the hole in the plastic bottle and completely prevent water leakage, indicating that the LTF bioadhesive could be incorporated with rigid backings to obtain adhesive tapes for enhanced mechanical strength. Importantly, it still had an excellent underwater adhesion even after 24 h (Figure 2c and Video S3), and long-term adhesion stability was desired in practical applications. Moreover, LTF supramolecular adhesive also had good adhesion to other tissues, such as stomach, heart, liver, and kidney (Figure 2d). The lap shear strength of these tissues was all beyond 20 kPa, which was about 2-fold stronger than the gold standard, a commercially available biological fibrin sealant used in clinical care (Figure 2e).[52−54] Meanwhile, in the bursting pressure test, LTF supramolecular bioadhesive also showed good water-proof performance for different tissues (Figure 2f).[30] In addition, as shown in Figure 2g, the adhesion force of the LTF supramolecular bioadhesive was tested by a texture analyzer and there was no significant difference in the adhesion force (around 0.8 N) in both dry and underwater environments, this might be attributed to the amphiphilicity of LA and the catechol chemistry of TA in the LTF bioadhesive system.[16,24] The robust and stable adhesion capacity for various tissue substrates in different environments revealed that the LTF bioadhesives could potentially be used in a wide range of biomedical applications.

3.2. Cytocompatibility of the LTF Supramolecular Bioadhesive *In Vitro*. The biosafety of bioadhesives is a key factor when applying them in clinical applications.[55] L929 cells were selected to verify the biosafety of the LTF supramolecular bioadhesive.[56] As shown in Figure 3a, the LTF bioadhesive showed excellent cytocompatibility after coculturing with L929 with different concentrations (the cell viability >90%). The value of OD_{450} was gradually increased with the time of coculture (Figure 3b), indicating the LTF bioadhesive could promote the proliferation of L929 cells, which was beneficial to wound healing.[57] In addition, the dead/living staining images of L929 cells of all experimental groups were similar to that of the control group on the first day and seventh day, and obvious cell proliferation was observed on the seventh day (Figure 3c). Moreover, the morphology of L929 cells had no significant difference between all groups on the first day, as the cells presented a typical spindle state (Figure 3d).[32] These results showed that the LTF supramolecular bioadhesive had good

https://doi.org/10.1021/acsami.2c17415
ACS Appl. Mater. Interfaces XXXX, XXX, XXX−XXX

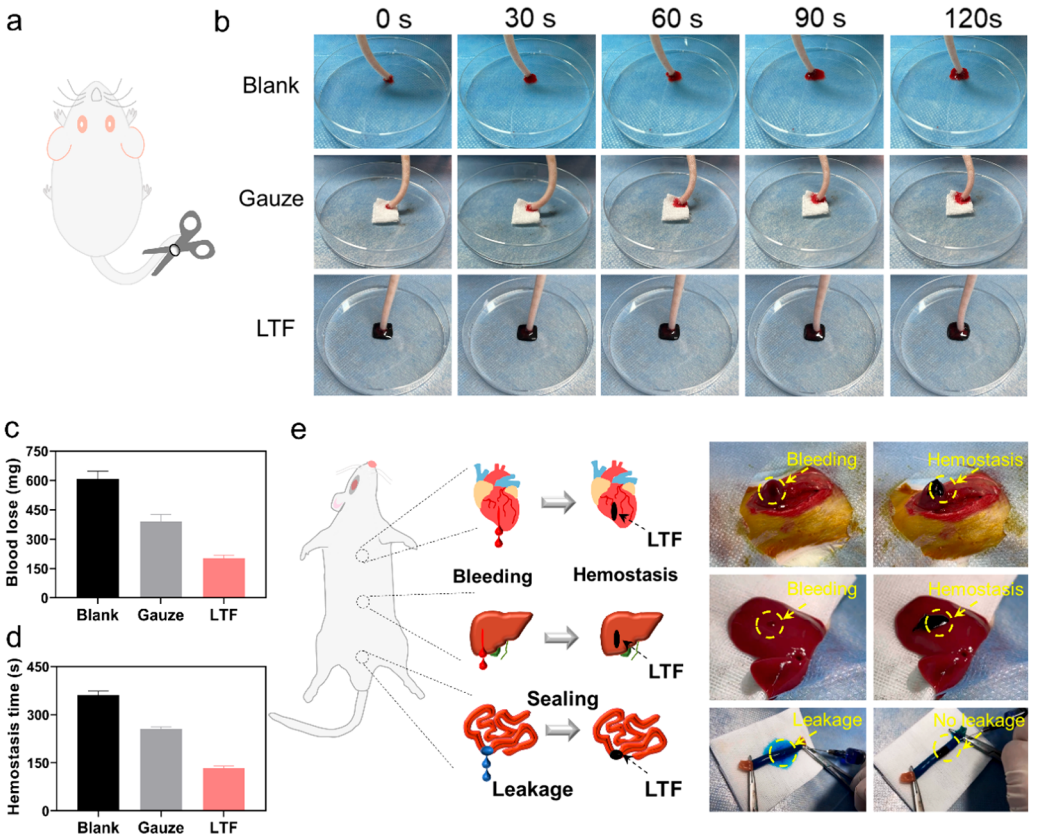

Figure 5. Hemostatic and sealing abilities. (a) Schematic diagram and (b) photographs of hemostatic property of the LTF supramolecular bioadhesive for the cut rat tail. (c) Blood loss and (d) hemostasis time of the LTF supramolecular bioadhesive for the cut rat tail. The values are presented as the mean ± SD (e) Hemostatic and sealing abilities of the LTF supramolecular bioadhesive for the rat heart, liver and intestine.

cytocompatibility and had great potential to be applied in biomedical fields.

3.3. Photothermal and Antibacterial Properties of the LTF Supramolecular Bioadhesive *In Vitro*. Previous studies had shown that TA and Fe^{3+} could form a complex exhibiting good photothermal properties by the catechol–metal coordination bonds, which suggested that the LTF supramolecular bioadhesive had the potential to be applied for photothermal antibiosis in biomedicine fields, especially for infectious wound management.[13,26,27]

In order to evaluate the photothermal properties of the LTF supramolecular bioadhesive, the LTF bioadhesive was continuously irradiated for 5 min under different power densities of 808 nm NIR. With increasing the power density, the temperature of the LTF bioadhesive increased gradually (Figure 4a). Bacteria could be killed when the temperature was greater than 50 °C,[58−60] and the temperature of the bioadhesive rapidly reached over 50 °C in 30 s under NIR irradiation and then stabilized when the power density was 1.5 W cm^{-2}. Therefore, the power density was set as 1.5 W cm^{-2} in the following sections as a suitable condition. In addition, the temperature of the LTF bioadhesive in the thermal images showed the same tendency (Figure 4b). Importantly, the LTF bioadhesive was thermally activated repeatedly and steadily after 5 times on/off cycle of NIR irradiation as there was no significant difference in the maximum heating temperature (Figure 4c).

The photothermal antibacterial properties of the LTF bioadhesive were assessed by *S. aureus* and *E. coli* (Figure 4d). As shown in Figure 4e, there were mild antibacterial properties of the LTF bioadhesive against *E. coli* (28.72 ± 3.59%) and *S. aureus* (30.95 ± 0.52%) due to the inherent antibacterial properties of TA.[61,62] The antibacterial capacity of the LTF bioadhesive increased significantly after NIR irradiation and showed excellent photothermal antibacterial properties against *E. coli* (100.45 ± 1.09%) and *S. aureus* (99.02 ± 1.07%). In addition, for the group with the LTF bioadhesive, there was no colony of *S. aureus* and *E. coli* formation on the solid agar plate after NIR irradiation (Figure 4f). These results further confirmed that LTF supramolecular bioadhesive had excellent photothermal antibacterial properties.

3.4. Hemostatic and Sealing Properties of the LTF Supramolecular Bioadhesive *In Vivo* and *In Vitro*. The instant waterproof ability, tissue adhesion performance, and cytocompatibility of the LTF supramolecular bioadhesive *in vitro* all showed its potential in biomedical fields, especially for hemostasis, sealing, wound closure, and wound healing.[15,35,36] As shown in Figure 5a, in the tail hemostasis experiment of Sprague–Dawley (SD) rats, compared with the blank group and the gauze group, the LTF bioadhesive exhibited an obviously better hemostatic performance (Figure 5b). In addition, the blood loss of the group treated with the LTF bioadhesive (202.17 ± 15.57 mg) was significantly less than the blank group and the gauze group (607.60 ± 38.85 mg and 389.53 ± 36.97 mg, respectively) (Figure 5c). The hemostasis time of the group treated with the LTF bioadhesive (133 ± 6.56 s) was also obviously shorter than the blank group and the gauze group (361.33 ± 11.93 s and 256.00 ± 6.24 s, respectively) (Figure 5d). The excellent hemostasis capacity of

https://doi.org/10.1021/acsami.2c17415
ACS Appl. Mater. Interfaces XXXX, XXX, XXX−XXX

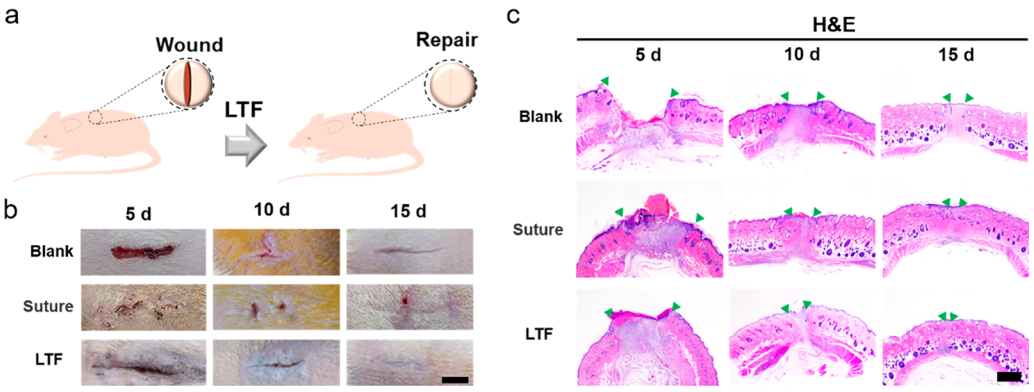

Figure 6. *In vivo* wound closure with the LTF supramolecular bioadhesive. (a) Schematic diagram of the *in vivo* wound closure abilities with the LTF supramolecular bioadhesive. (b) Photographs of wound closure with different treatments at different periods. Scale bar = 1 cm. (c) H&E staining images of the wound closure section on the days 5, 10, and 15, respectively. The wound edges are marked with green triangles. Scale bar = 1 mm.

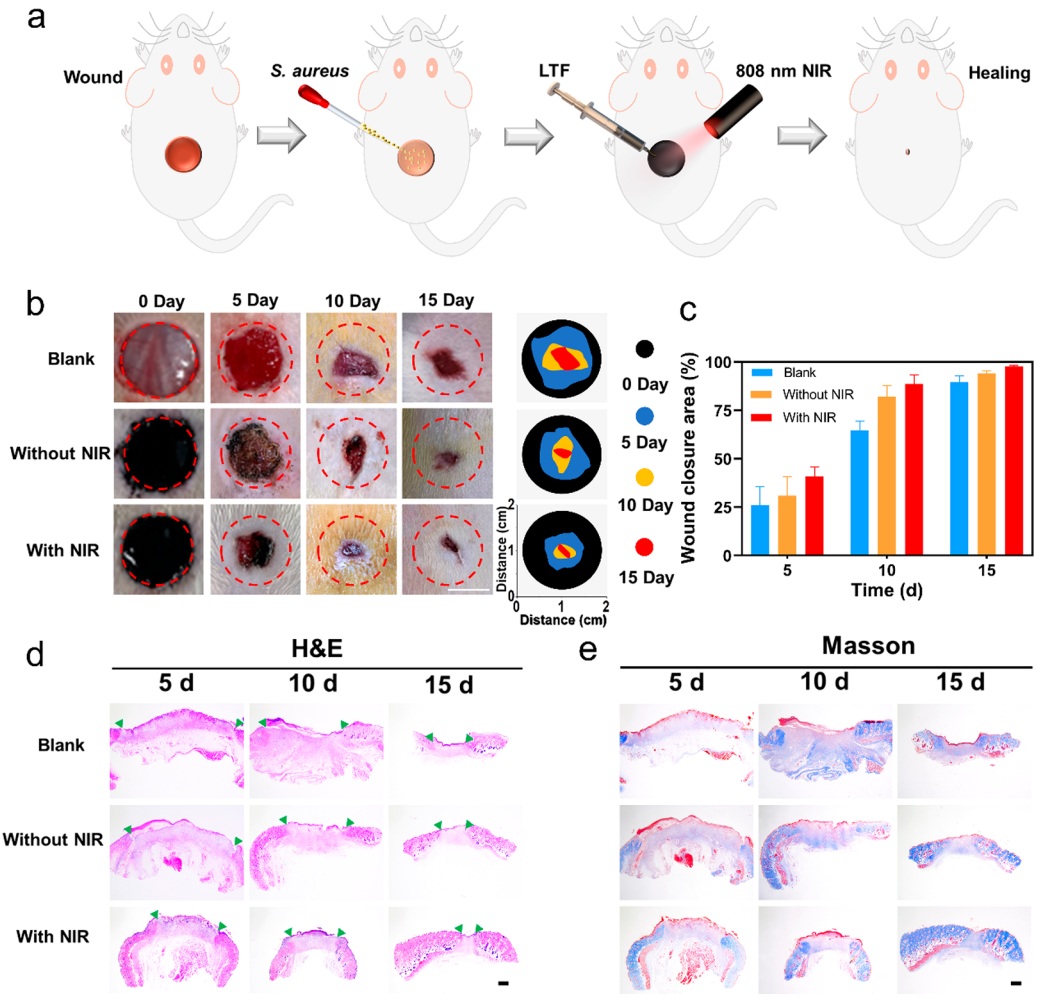

Figure 7. *In vivo* full-thickness skin wound healing with the LTF supramolecular bioadhesive. (a) Schematic diagram of the full-thickness skin wound-healing abilities of the LTF supramolecular bioadhesive. (b) Photographs of the wound healing with different treatments at different periods. Scale bar = 1 cm. (c) Average ratio of wound closure area on days 5, 10, and 15, respectively. The values are presented as the mean ± SD. (d) H&E and (e) Masson staining images of the wound section on days 5, 10, and 15, respectively. The wound edges are marked with green triangles. Scale bar = 1 mm.

the LTF bioadhesive was further displayed on the bleeding sites of the heart and liver of SD rats (Figure 5e and Videos S4 and S5).[34,35,63] Moreover, the leaking incision site of the intestine could also be well sealed with the LTF bioadhesive as the bright blue-stained normal saline would no longer leak from the incision site (Figure 5e and Video S6).[36] This was most likely mainly attributed to the strong interactions between the phenolic moiety of TA in the LTF bioadhesive

https://doi.org/10.1021/acsami.2c17415
ACS Appl. Mater. Interfaces XXXX, XXX, XXX−XXX

and nucleophiles in blood proteins that accelerate platelet aggregation and activation of clotting factors. In addition, the LTF bioadhesive with good wettability and adhesion property in the bleeding site could act as a physical barrier to prevent blood from leaking out and achieve the nonpressing hemostatic and sealing performance, which is beneficial to wound healing.[15,34]

3.5. Free Radical Scavenging Performance of the LTF Supramolecular Bioadhesive. In the process of wound healing, excessive reactive oxygen species (ROS) will be produced around the wound due to the local bacterial infection and the local wound microenvironment. The excessive production of ROS will greatly hinder wound healing.[64,65] Therefore, we assessed the DPPH radical removal performance of the LTF supramolecular bioadhesive. As shown in Figure S9, the LTF bioadhesive had a concentration-dependent DPPH radical removal property, and when the concentration of the LTF bioadhesive was higher than 0.5 mg mL^{-1}, it exhibited excellent DPPH radical scavenging performance (>90%). This may be attributed to the antioxidant property of TA in the LTF supramolecular bioadhesive.[33]

The good biocompatibility and free radical removal property of the LTF supramolecular bioadhesive would further benefit its application in wound healing.[65] Therefore, two rat wound models were selected for assessing the practical value of the LTF bioadhesive.

3.6. Wound Closure Ability of the LTF Supramolecular Bioadhesive for the Linear Wound *In Vivo*. In the repair experiment of linear skin wounds on the back of SD rats (Figure 6a), the LTF supramolecular bioadhesive could close the linear wound efficiently in the early stage of wound healing. In the later stage (Figure 6b), the bioadhesive can effectively promote wound healing and induce less scar than in other groups.[34] According to the results of hematoxylin and eosin (H&E) staining (Figure 6c), on day 15, it could be seen that the repair of the tissue and the hair follicles around the wound after treatment by the LTF bioadhesive was relatively complete and the distance from the edge of the wound was obviously shorter than that of other groups, which further proved that the LTF bioadhesive could promote the wound healing (Figure 6c).[66]

3.7. Full-Thickness Skin Wound Healing Capacities of the LTF Supramolecular Bioadhesive *In Vivo*. A full-thickness skin defect wound model with *S. aureus* infection was established on the back of SD rats to further evaluate the photothermal antibacterial and wound healing performance of the LTF supramolecular bioadhesive (Figure 7a).[26,43,67] As shown in Figure 7b,c, the wound size gradually decreased with time for all tested groups. Notably, the wound treated with the LTF bioadhesive under 0 had the fastest wound healing rate. Interestingly, the wound treated with the LTF bioadhesive was better than that of the blank group, which may be explained by the inherent anti-inflammatory and antibacterial effects of TA and LA. In addition, the histological analysis in skin tissues around the wound section using H&E staining and Masson's staining was used to further evaluate the healing outcomes. On day 15 (Figure 7d), the wound treated with the LTF bioadhesive under NIR irradiation had a better and relatively complete wound healing than other groups as more new tissues, more collagen deposition and regenerated hair follicles were generated around the wound. These results strongly suggested that the LTF bioadhesive could play a key role in promoting the healing of infectious wounds.[68,69]

4. CONCLUSIONS

In this work, natural small biological molecules were explored to fabricate a supramolecular bioadhesive with a combination of mechanical, biological, and innate synergistic antibacterial properties, via a green and facile way for wound management. The self-healing supramolecular bioadhesive with good injectability, biocompatibility, and free radical scavenging ability can form stable and robust adhesion to tissues and perform efficient hemostasis and synergistic photothermal and polyphenol antibacterial effects to enhance healing. It provides an easy-to-use alternative nonpharmacological wound management strategy, especially for minimally invasive surgeries and infectious cases. The supramolecular bioadhesive may also be useful as a drug carrier and a multifunctional component of soft-robotics-based therapies.

■ ASSOCIATED CONTENT

Supporting Information

The Supporting Information is available free of charge at https://pubs.acs.org/doi/10.1021/acsami.2c17415.

Injectability of the LTF supramolecular bioadhesive on the fresh porcine skin underwater (MP4)

Sealing ability of the LTF supramolecular bioadhesive to the plastic bottle filled with water (MP4)

Adhesion of the LTF supramolecular bioadhesive under underwater (MP4)

Hemostatic properties of the LTF supramolecular bioadhesive to the SD rat heart *in vivo* (MP4)

Hemostatic properties of the LTF supramolecular bioadhesive to the SD rat liver *in vivo* (MP4)

Sealing ability of the LTF supramolecular bioadhesive to the SD rat intestine *in vitro* (MP4)

^{1}H and ^{13}C NMR, FT-IR, XRD, DSC, SEM, and rheological results of LFT bioadhesive; the photographs of self-healing tests and the results of radical scavenging activity experiments (PDF)

■ AUTHOR INFORMATION

Corresponding Authors

Jun Luo − *College of Polymer Science and Engineering, State Key Laboratory of Polymer Materials Engineering, Sichuan University, Chengdu 610065, P.R. China*; Email: luojuncd@scu.edu.cn

Jianshu Li − *College of Polymer Science and Engineering, State Key Laboratory of Polymer Materials Engineering and Med-X Center for Materials, Sichuan University, Chengdu 610065, P.R. China; State Key Laboratory of Oral Diseases, West China Hospital of Stomatology, Sichuan University, Chengdu 610041, China;* orcid.org/0000-0002-1522-7326; Email: jianshu_li@scu.edu.cn

Authors

Xiang Ke − *College of Polymer Science and Engineering, State Key Laboratory of Polymer Materials Engineering, Sichuan University, Chengdu 610065, P.R. China; College of Chemistry and Chemical Engineering, Guizhou University, Guiyang 550025, P.R. China*

Shuxian Tang − *College of Polymer Science and Engineering, State Key Laboratory of Polymer Materials Engineering, Sichuan University, Chengdu 610065, P.R. China*

https://doi.org/10.1021/acsami.2c17415
ACS Appl. Mater. Interfaces XXXX, XXX, XXX−XXX

Hao Wang − *College of Polymer Science and Engineering, State Key Laboratory of Polymer Materials Engineering, Sichuan University, Chengdu 610065, P.R. China*
Yusong Cai − *College of Polymer Science and Engineering, State Key Laboratory of Polymer Materials Engineering, Sichuan University, Chengdu 610065, P.R. China*
Zhiyun Dong − *College of Polymer Science and Engineering, State Key Laboratory of Polymer Materials Engineering, Sichuan University, Chengdu 610065, P.R. China*
Mingjing Li − *College of Polymer Science and Engineering, State Key Laboratory of Polymer Materials Engineering, Sichuan University, Chengdu 610065, P.R. China*
Jiaojiao Yang − *State Key Laboratory of Oral Diseases, West China Hospital of Stomatology, Sichuan University, Chengdu 610041, China;* orcid.org/0000-0002-8611-4089
Xinyuan Xu − *College of Polymer Science and Engineering, State Key Laboratory of Polymer Materials Engineering, Sichuan University, Chengdu 610065, P.R. China*

Complete contact information is available at: https://pubs.acs.org/10.1021/acsami.2c17415

Notes

The authors declare no competing financial interest.

■ ACKNOWLEDGMENTS

Financial support from the National Natural Science Foundation of China (Grant Nos. 51925304, 51903175, and 52073191) is gratefully acknowledged. The authors also acknowledge the Shiyanjia Lab (www.shiyanjia.com) for the ^{1}H NMR and ^{13}C NMR measurements.

■ REFERENCES

(1) Weiser, T. G.; Regenbogen, S. E.; Thompson, K. D.; Haynes, A. B.; Lipsitz, S. R.; Berry, W. R.; Gawande, A. A. An Estimation of the Global Volume of Surgery: a Modelling Strategy based on Available Data. *Lancet* **2008**, *372*, 139−144.
(2) Gurtner, G. C.; Werner, S.; Barrandon, Y.; Longaker, M. T. Wound Repair and Regeneration. *Nature* **2008**, *453*, 314−321.
(3) Annabi, N.; Tamayol, A.; Shin, S. R.; Ghaemmaghami, A. M.; Peppas, N. A.; Khademhosseini, A. Surgical Materials: Current Challenges and Nano-enabled Solutions. *Nano Today* **2014**, *9*, 574−589.
(4) Artzi, N. Sticking with the Pattern for a Safer Glue. *Sci. Transl. Med.* **2013**, *5*, 205ec161.
(5) Ghobril, C.; Grinstaff, M. W. The Chemistry and Engineering of Polymeric Hydrogel Adhesives for Wound Closure: A Tutorial. *Chem. Soc. Rev.* **2015**, *44*, 1820−1835.
(6) Nam, S.; Mooney, D. Polymeric Tissue Adhesives. *Chem. Rev.* **2021**, *121*, 11336−11384.
(7) Cui, C.; Liu, W. Recent Advances in Wet Adhesives: Adhesion Mechanism, Design Principle and Applications. *Prog. Polym. Sci.* **2021**, *116*, 101388.
(8) Chen, X.; Yuk, H.; Wu, J.; Nabzdyk, C. S.; Zhao, X. Instant Tough Bioadhesive with Triggerable Benign Detachment. *Proc. Natl. Acad. Sci. U. S. A.* **2020**, *117*, 15497−15503.
(9) Li, J.; Celiz, A. D.; Yang, J.; Yang, Q.; Wamala, I.; Whyte, W.; Seo, B. R.; Vasilyev, N. V.; Vlassak, J. J.; Suo, Z.; Mooney, D. J. Tough Adhesives for Diverse Wet Surfaces. *Science* **2017**, *357*, 378−381.
(10) Li, S.; Dong, S.; Xu, W.; Tu, S.; Yan, L.; Zhao, C.; Ding, J.; Chen, X. Antibacterial Hydrogels. *Adv. Sci.* **2018**, *5*, 1700527.
(11) Xin, Q.; Shah, H.; Nawaz, A.; Xie, W.; Akram, M. Z.; Batool, A.; Tian, L.; Jan, S. U.; Boddula, R.; Guo, B.; Liu, Q.; Gong, J. R. Antibacterial Carbon-Based Nanomaterials. *Adv. Mater.* **2019**, *31*, 1804838.
(12) Guo, J.; Sun, W.; Kim, J. P.; Lu, X.; Li, Q.; Lin, M.; Mrowczynski, O.; Rizk, E. B.; Cheng, J.; Qian, G.; Yang, J. Development of Tannin-Inspired Antimicrobial Bioadhesives. *Acta Biomater.* **2018**, *72*, 35−44.
(13) Liu, T.; Zhang, M.; Liu, W.; Zeng, X.; Song, X.; Yang, X.; Zhang, X.; Feng, J. Metal Ion/Tannic Acid Assembly as a Versatile Photothermal Platform in Engineering Multimodal Nanotheranostics for Advanced Applications. *ACS Nano* **2018**, *12*, 3917−3927.
(14) Luo, J.; Yang, J.; Zheng, X.; Ke, X.; Chen, Y.; Tan, H.; Li, J. A Highly Stretchable, Real-Time Self-Healable Hydrogel Adhesive Matrix for Tissue Patches and Flexible Electronics. *Adv. Healthcare Mater.* **2020**, *9*, 1901423.
(15) Zhu, J.; Zhong, K.; Zong, Y.; Wang, S.; Yang, H.; Zhen, L.; Tao, S.; Sun, L.; Yang, J.; Li, J. A Mussel-inspired Wet-adhesion Hydrogel with Hemostasis and Local Anti-inflammation for Managing the Development of Acute Wounds. *Mater. Des.* **2022**, *213*, 110347.
(16) Zhao, Q.; Lee, D. W.; Ahn, B. K.; Seo, S.; Kaufman, Y.; Israelachvili, J. N.; Waite, J. H. Underwater Contact Adhesion and Microarchitecture in Polyelectrolyte Complexes Actuated by Solvent Exchange. *Nat. Mater.* **2016**, *15*, 407−412.
(17) Ke, X.; Dong, Z.; Tang, S.; Chu, W.; Zheng, X.; Zhen, L.; Chen, X.; Ding, C.; Luo, J.; Li, J. A Natural Polymer Based Bioadhesive with Self-healing Behavior and Improved Antibacterial Properties. *Biomater. Sci.* **2020**, *8*, 4346−4357.
(18) Gan, D.; Xing, W.; Jiang, L.; Fang, J.; Zhao, C.; Ren, F.; Fang, L.; Wang, K.; Lu, X. Plant-inspired Adhesive and Tough Hydrogel Based on Ag-Lignin Nanoparticles-Triggered Dynamic Redox Catechol Chemistry. *Nat. Commun.* **2019**, *10*, 1487.
(19) Ke, X.; Tang, S.; Dong, Z.; Wang, H.; Xu, X.; Qiu, R.; Yang, J.; Luo, J.; Li, J. A Silk Fibroin Based Bioadhesive with Synergistic Photothermal-reinforced Antibacterial Activity. *Int. J. Biol. Macromol.* **2022**, *209*, 608−617.
(20) Shi, C.-Y.; Zhang, Q.; Tian, H.; Qu, D.-H. Supramolecular Adhesive Materials from Small-molecule Self-assembly. *SmartMat* **2020**, *1*, No. e1012.
(21) Cui, C.; Liu, B.; Wu, T.; Liu, Y.; Fan, C.; Xu, Z.; Yao, Y.; Liu, W. A Hyperbranched Polymer Elastomer-based Pressure Sensitive Adhesive. *J. Mater. Chem. A* **2022**, *10*, 1257−1269.
(22) Tardy, B. L.; Mattos, B. D.; Otoni, C. G.; Beaumont, M.; Majoinen, J.; Kämäräinen, T.; Rojas, O. J. Deconstruction and Reassembly of Renewable Polymers and Biocolloids into Next Generation Structured Materials. *Chem. Rev.* **2021**, *121*, 14088−14188.
(23) Shi, C.-Y.; Zhang, Q.; Wang, B.-S.; Chen, M.; Qu, D.-H. Intrinsically Photopolymerizable Dynamic Polymers Derived from a Natural Small Molecule. *ACS Appl. Mater. Interfaces* **2021**, *13*, 44860−44867.
(24) Ambrosi, N.; Guerrieri, D.; Caro, F.; Sanchez, F.; Haeublein, G.; Casadei, D.; Incardona, C.; Chuluyan, E. Alpha Lipoic Acid: A Therapeutic Strategy that Tend to Limit the Action of Free Radicals in Transplantation. *Int. J. Mol. Sci.* **2018**, *19*, 102.
(25) Ke, X.; Tang, S.; Dong, Z.; Ren, K.; Yu, P.; Xu, X.; Yang, J.; Luo, J.; Li, J. An Instant, Repeatable and Universal Supramolecular Adhesive based on Natural Small Molecules for Dry/Wet Environments. *Chem. Eng. J.* **2022**, *442*, 136206.
(26) Yu, Y.; Li, P.; Zhu, C.; Ning, N.; Zhang, S.; Vancso, G. J. Multifunctional and Recyclable Photothermally Responsive Cryogels as Efficient Platforms for Wound Healing. *Adv. Funct. Mater.* **2019**, *29*, 1904402.
(27) Zhao, X.; Liang, Y.; Huang, Y.; He, J.; Han, Y.; Guo, B. Physical Double-Network Hydrogel Adhesives with Rapid Shape Adaptability, Fast Self-Healing, Antioxidant and NIR/pH Stimulus-Responsiveness for Multidrug-Resistant Bacterial Infection and Removable Wound Dressing. *Adv. Funct. Mater.* **2020**, *30*, 1910748.
(28) *ASTM F2255−05 Standard Test Method for Strength Properties of Tissue Adhesives in Lap-Shear by Tension Loading*; ASTM, 2015).
(29) Yang, J.; Chen, S.; Luo, J.; Persson, C.; Cölfen, H.; Welch, K.; Strømme, M. Multifunctional Polymer-Free Mineral Plastic Adhesives

Formed by Multiple Noncovalent Bonds. *ACS Appl. Mater. Interfaces* **2020**, *12*, 7403−7410.
(30) Azuma, K.; Nishihara, M.; Shimizu, H.; Itoh, Y.; Takashima, O.; Osaki, T.; Itoh, N.; Imagawa, T.; Murahata, Y.; Tsuka, T.; Izawa, H.; Ifuku, S.; Minami, S.; Saimoto, H.; Okamoto, Y.; Morimoto, M. Biological Adhesive Based on Carboxymethyl Chitin Derivatives and Chitin Nanofibers. *Biomaterials* **2015**, *42*, 20−29.
(31) Zhou, F.; Hong, Y.; Zhang, X.; Yang, L.; Li, J.; Jiang, D.; Bunpetch, V.; Hu, Y.; Ouyang, H.; Zhang, S. Tough Hydrogel with Enhanced Tissue Integration and In Situ Forming Capability for Osteochondral Defect Repair. *Appl. Mater. Today* **2018**, *13*, 32−44.
(32) Sun, H.; Zhang, M.; Liu, M.; Yu, Y.; Xu, X.; Li, J. Fabrication of Double-Network Hydrogels with Universal Adhesion and Superior Extensibility and Cytocompatibility by One-Pot Method. *Biomacromolecules* **2020**, *21*, 4699−4708.
(33) Ren, K.; Ke, X.; Chen, Z.; Zhao, Y.; He, L.; Yu, P.; Xing, J.; Luo, J.; Xie, J.; Li, J. Zwitterionic Polymer Modified Xanthan Gum with Collagen II-Binding Capability for Lubrication Improvement and ROS Scavenging. *Carbohydr. Polym.* **2021**, *274*, 118672.
(34) Bai, S.; Zhang, X.; Cai, P.; Huang, X.; Huang, Y.; Liu, R.; Zhang, M.; Song, J.; Chen, X.; Yang, H. A Silk-based Sealant with Tough Adhesion for Instant Hemostasis of Bleeding Tissues. *Nanoscale Horiz.* **2019**, *4*, 1333−1341.
(35) Wang, R.; Li, J.; Chen, W.; Xu, T.; Yun, S.; Xu, Z.; Xu, Z.; Sato, T.; Chi, B.; Xu, H. A Biomimetic Mussel-Inspired ε-Poly-l-lysine Hydrogel with Robust Tissue-Anchor and Anti-Infection Capacity. *Adv. Funct. Mater.* **2017**, *27*, 1604894.
(36) Hong, S.; Pirovich, D.; Kilcoyne, A.; Huang, C. H.; Lee, H.; Weissleder, R. Supramolecular Metallo-Bioadhesive for Minimally Invasive Use. *Adv. Mater.* **2016**, *28*, 8675−8680.
(37) Chen, C.; Yang, X.; Li, S.; Zhang, C.; Ma, Y.; Ma, Y.; Gao, P.; Gao, S.; Huang, X.-J. Tannic Acid-Thioctic Acid Hydrogel: A Novel Injectable Supramolecular Adhesive Gel for Wound Healing. *Green Chem.* **2021**, *23*, 1794.
(38) Zhang, Q.; Shi, C.-Y.; Qu, D.-H.; Long, Y.-T.; Feringa, B. L.; Tian, H. Exploring a Naturally Tailored Small Molecule for Stretchable, Self-healing, and Adhesive Supramolecular Polymers. *Sci. Adv.* **2018**, *4*, eaat8192.
(39) Deng, Y.; Zhang, Q.; Feringa, B. L.; Tian, H.; Qu, D.-H. Toughening a Self-Healable Supramolecular Polymer by Ionic Cluster-Enhanced Iron-Carboxylate Complexes. *Angew. Chem. In. Ed.* **2020**, *59*, 5278−5283.
(40) Dang, C.; Wang, M.; Yu, J.; Chen, Y.; Zhou, S.; Feng, X.; Liu, D.; Qi, H. Transparent, Highly Stretchable, Rehealable, Sensing, and Fully Recyclable Ionic Conductors Fabricated by One-Step Polymerization Based on a Small Biological Molecule. *Adv. Funct. Mater.* **2019**, *29*, 1902467.
(41) Zhang, D.; Xu, Z.; Li, H.; Fan, C.; Cui, C.; Wu, T.; Xiao, M.; Yang, Y.; Yang, J.; Liu, W. Fabrication of Strong Hydrogen-Bonding Induced Coacervate Adhesive Hydrogels with Antibacterial and Hemostatic Activities. *Biomater. Sci.* **2020**, *8*, 1455−1463.
(42) Kim, S. H.; Kim, K.; Kim, B. S.; An, Y. H.; Lee, U. J.; Lee, S. H.; Kim, S. L.; Kim, B. G.; Hwang, N. S. Fabrication of Polyphenol-Incorporated Anti-Inflammatory Hydrogel via High-affinity Enzymatic Crosslinking for Wet Tissue Adhesion. *Biomaterials* **2020**, *242*, 119905.
(43) Qu, J.; Zhao, X.; Liang, Y.; Zhang, T.; Ma, P. X.; Guo, B. Antibacterial Adhesive Injectable Hydrogels with Rapid Self-Healing, Extensibility and Compressibility as Wound Dressing for Joints Skin Wound Healing. *Biomaterials* **2018**, *183*, 185−199.
(44) Zhang, K.; Chen, X.; Xue, Y.; Lin, J.; Liang, X.; Zhang, J.; Zhang, J.; Chen, G.; Cai, C.; Liu, J. Tough Hydrogel Bioadhesives for Sutureless Wound Sealing, Hemostasis and Biointerfaces. *Adv. Funct. Mater.* **2022**, *32*, 2111465.
(45) Chen, X.; Zhang, J.; Chen, G.; Xue, Y.; Zhang, J.; Liang, X.; Lei, I. M.; Lin, J.; Xu, B. B.; Liu, J. Hydrogel Bioadhesives with Extreme Acid-Tolerance for Gastric Perforation Repairing. *Adv. Funct. Mater.* **2022**, *32*, 2202285.
(46) Xu, Y.; Rothe, R.; Voigt, D.; Hauser, S.; Cui, M.; Miyagawa, T.; Patino Gaillez, M.; Kurth, T.; Bornhäuser, M.; Pietzsch, J.; Zhang, Y. Convergent Synthesis of Diversified Reversible Network Leads to Liquid Metal-containing Conductive Hydrogel Adhesives. *Nat. Commun.* **2021**, *12*, 2407.
(47) Hu, J.; Zheng, Z.; Liu, C.; Hu, Q.; Cai, X.; Xiao, J.; Cheng, Y. A pH-Responsive Hydrogel with Potent Antibacterial Activity Against both Aerobic and Anaerobic Pathogens. *Biomater. Sci.* **2019**, *7*, 581−584.
(48) A, S.; Xu, Q.; Johnson, M.; Creagh-Flynn, J.; Venet, M.; Zhou, D.; Lara-Sáez, I.; Tai, H.; Wang, W. An Injectable Multi-Responsive Hydrogel as Self-Healable and On-Demand Dissolution Tissue Adhesive. *Appl. Mater. Today* **2021**, *22*, 100967.
(49) Cao, J.; Wu, P.; Cheng, Q.; He, C.; Chen, Y.; Zhou, J. Ultrafast Fabrication of Self-Healing and Injectable Carboxymethyl Chitosan Hydrogel Dressing for Wound Healing. *ACS Appl. Mater. Interfaces* **2021**, *13*, 24095−24105.
(50) Kord Forooshani, P.; Lee, B. P. Recent Approaches in Designing Bioadhesive Materials Inspired by Mussel Adhesive Protein. *J. Polyme. Sci. Part A. Polym. Chem.* **2017**, *55*, 9−33.
(51) Xu, X.; Xia, X.; Zhang, K.; Rai, A.; Li, Z.; Zhao, P.; Wei, K.; Zou, L.; Yang, B.; Wong, W.-K.; Chiu, P.W.-Y. Bioadhesive Hydrogels Demonstrating pH-independent and Ultrafast Gelation Promote Gastric Ulcer Healing in Pigs. *Sci. Transl. Med.* **2020**, *12*, eaba8014.
(52) Mehdizadeh, M.; Weng, H.; Gyawali, D.; Tang, L.; Yang, J. Injectable Citrate-Based Mussel-Inspired Tissue Bioadhesives with High Wet Strength for Sutureless Wound Closure. *Biomaterials* **2012**, *33*, 7972−7983.
(53) Su, X.; Luo, Y.; Tian, Z.; Yuan, Z.; Han, Y.; Dong, R.; Xu, L.; Feng, Y.; Liu, X.; Huang, J. Ctenophore-Inspired Hydrogels for Efficient and Repeatable Underwater Specific Adhesion to Biotic Surfaces. *Mater. Horiz.* **2020**, *7*, 2651−2661.
(54) Lang, N.; Pereira, M. J.; Lee, Y.; Friehs, I.; Vasilyev, N. V.; Feins, E. N.; Ablasser, K.; O'Cearbhaill, E. D.; Xu, C.; Fabozzo, A.; et al. A Blood-Resistant Surgical Glue for Minimally Invasive Repair of Vessels and Heart Defects. *Sci. Transl. Med.* **2014**, *6*, 218ra216.
(55) Zhu, W.; Chuah, Y. J.; Wang, D. A. Bioadhesives for Internal Medical Applications: A Review. *Acta Biomater.* **2018**, *74*, 1−16.
(56) Jablonská, E.; Horkavcová, D.; Rohanová, D.; Brauer, D. S. A Review of In Vitro Cell Culture Testing Methods for Bioactive Glasses and Other Biomaterials for Hard Tissue Regeneration. *J. Mater. Chem. B* **2020**, *8*, 10941−10953.
(57) Yu, P.; Xie, J.; Chen, Y.; Liu, J.; Liu, Y.; Bi, B.; Luo, J.; Li, S.; Jiang, X.; Li, J. A Thermo-Sensitive Injectable Hydroxypropyl Chitin Hydrogel for Sustained Salmon Calcitonin Release with Enhanced Osteogenesis and Hypocalcemic Effects. *J. Mater. Chem. B* **2020**, *8*, 270−281.
(58) Liang, Y.; Zhao, X.; Hu, T.; Chen, B.; Yin, Z.; Ma, P. X.; Guo, B. Adhesive Hemostatic Conducting Injectable Composite Hydrogels with Sustained Drug Release and Photothermal Antibacterial Activity to Promote Full-Thickness Skin Regeneration During Wound Healing. *Small* **2019**, *15*, No. 1900046.
(59) Tan, L.; Li, J.; Liu, X.; Cui, Z.; Yang, X.; Zhu, S.; Li, Z.; Yuan, X.; Zheng, Y.; Yeung, K. W. K.; et al. Rapid Biofilm Eradication on Bone Implants Using Red Phosphorus and Near-Infrared Light. *Adv. Mater.* **2018**, *30*, No. 1801808.
(60) Yang, Y.; Wu, X.; He, C.; Huang, J.; Yin, S.; Zhou, M.; Ma, L.; Zhao, W.; Qiu, L.; Cheng, C.; Zhao, C. Metal-Organic Framework/Ag-Based Hybrid Nanoagents for Rapid and Synergistic Bacterial Eradication. *ACS Appl. Mater. Interfaces* **2020**, *12*, 13698−13708.
(61) Sahiner, N.; Sagbas, S.; Sahiner, M.; Silan, C.; Aktas, N.; Turk, M. Biocompatible and Biodegradable Poly(Tannic Acid) Hydrogel with Antimicrobial and Antioxidant Properties. *Int. J. Biol. Macromol.* **2016**, *82*, 150−159.
(62) Xu, L. Q.; Neoh, K.-G.; Kang, E.-T. Natural Polyphenols as Versatile Platforms for Material Engineering and Surface Functionalization. *Prog. Polym. Sci.* **2018**, *87*, 165−196.
(63) Shin, J.; Lee, J. S.; Lee, C.; Park, H.-J.; Yang, K.; Jin, Y.; Ryu, J. H.; Hong, K. S.; Moon, S.-H.; Chung, H.-M.; et al. Tissue Adhesive

https://doi.org/10.1021/acsami.2c17415
ACS Appl. Mater. Interfaces XXXX, XXX, XXX−XXX

Catechol-Modified Hyaluronic Acid Hydrogel for Effective, Minimally Invasive Cell Therapy. *Adv. Funct. Mater.* **2015**, *25*, 3814−3824.
(64) Zhang, W.; Zhang, Y.; Li, X.; Cao, Z.; Mo, Q.; Sheng, R.; Ling, C.; Chi, J.; Yao, Q.; Chen, J.; Wang, H. Multifunctional Polyphenol-based Silk Hydrogel Alleviates Oxidative Stress and Enhances Endogenous Regeneration of Osteochondral Defects. *Mater. Today Bio.* **2022**, *14*, 100251.
(65) Sun, C.; Zeng, X.; Zheng, S.; Wang, Y.; Li, Z.; Zhang, H.; Nie, L.; Zhang, Y.; Zhao, Y.; Yang, X. Bio-adhesive Catechol-modified Chitosan Wound Healing Hydrogel Dressings through Glow Discharge Plasma Technique. *Chem. Eng. J.* **2022**, *427*, 130843.
(66) Blacklow, S. O.; Li, J.; Freedman, B. R.; Zeidi, M.; Chen, C.; Mooney, D. J. Bioinspired Mechanically Active Adhesive Dressings to Accelerate Wound Closure. *Sci. Adv.* **2019**, *5*, eaaw3963.
(67) Gao, L.; Zhou, Y.; Peng, J.; Xu, C.; Xu, Q.; Xing, M.; Chang, J. A Novel Dual-Adhesive and Bioactive Hydrogel Activated by Bioglass for Wound Healing. *NPG Asia Mater.* **2019**, *11*, 66.
(68) Zhou, J.; Wu, Y.; Zhang, X.; Lai, J.; Li, Y.; Xing, J.; Teng, L.; Chen, J. Enzyme Catalyzed Hydrogel as Versatile Bioadhesive for Tissue Wound Hemostasis, Bonding, and Continuous Repair. *Biomacromolecules* **2021**, *22*, 1346−1356.
(69) Feng, L.; Shi, W.; Chen, Q.; Cheng, H.; Bao, J.; Jiang, C.; Zhao, W.; Zhao, C. Smart Asymmetric Hydrogel with Integrated Multi-Functions of NIR-Triggered Tunable Adhesion, Self-Deformation, and Bacterial Eradication. *Adv. Healthcare Mater.* **2021**, *10*, 2100784.

https://doi.org/10.1021/acsami.2c17415
ACS Appl. Mater. Interfaces XXXX, XXX, XXX−XXX